Iran J Nucl Med. 2025;33(2):103-115 [Serial No. 65]

Homepage: https://irjnm.tums.ac.ir/

ORIGINAL RESEARCH ARTICLE

Optimization of image reconstruction protocol in neurological [^{18}F]FDG brain PET imaging using BGO-based Discovery IQ scanner

Mahsa Asami[1], Farahnaz Aghahosseini[2], Saeed Farzanehfar[2], Pardis Ghafarian[3,4], Yalda Salehi[2], Mohammad Reza Ay[1,5], Nima Kasraie[6], Peyman Sheikhzadeh[1,2,7*]

[1]Department of Medical Physics and Biomedical Engineering, School of Medicine, Tehran University of Medical Sciences, Tehran, Iran
[2]Department of Nuclear Medicine, Imam Khomeini Hospital Complex, Tehran University of Medical Sciences, Tehran, Iran
[3]Chronic Respiratory Diseases Research Center, National Research Institute of Tuberculosis and Lung Diseases, Shahid Beheshti University of Medical Sciences, Tehran, Iran
[4]PET/CT and Cyclotron Center, Masih Daneshvari Hospital, Shahid Beheshti University of Medical Sciences, Tehran, Iran
[5]Research Center for Molecular and Cellular Imaging, Tehran University of Medical Sciences, Tehran, Iran
[6]Department of Radiology, UT Southwestern Medical Center, Dallas, TX 75390-9071, USA
[7]Research Center for Nuclear Medicine, Tehran University of Medical Sciences, Tehran, Iran

ARTICLE INFO

Article History:
Received: 12 February 2025
Revised: 29 May 2025
Accepted: 31 May 2025
Published Online: 19 June 2025

Keyword:
PET/CT
Q.Clear
Bayesian penalized likelihood
Image quality
Optimization

*Corresponding Author:
Dr. Peyman Sheikhzadeh
Address: Department of Nuclear Medicine, Tehran University of Medical Sciences, Tehran, Iran
Email: sheikhzadeh-p@sina.tums.ac.ir

ABSTRACT

Introduction: Since the Ordered Subset Expectation Maximization (OSEM) and Q.Clear algorithm each have advantages and disadvantages, we aimed to determine the optimal values of reconstruction protocols to achieve the best diagnostic parameters for the neurological PET brain images of BGO-based PET/CT scanners.

Methods: Images of point sources, as well as Hoffman and Carlson phantoms filled with [^{18}F]FDG radiopharmaceutical, were acquired using a PET/CT scanner. In OSEM, images were reconstructed with multiple iterations and subsets, applying 3.2 mm or 6.4 mm Gaussian filters, with PSF recovery enabled. For comparison, one reconstruction was done without PSF recovery using Iteration-Subset=12–12. In Q.Clear, β values from 50 to 500 in 50-step increments were used for reconstruction. Parameters such as FWHM, COV and modified RC were evaluated. A cost function identified the best results, which were blindly assessed by two nuclear medicine experts for noise, contrast, and overall image quality.

Results: Quantitatively, β=50-200 and Iteration-Subset=20-12 were the parameters whose Cost Function values were higher than Iteration-Subset =12-12, which was routinely used to reconstruct brain images in our center. Visual evaluations show that β=200 has the lowest noise and the lowest contrast and evaluators gave the highest score for overall image quality to β=200 and β=150. This study has evaluated β=200 and β=150 as optimal for reconstructing brain images.

Conclusion: This study investigated the different reconstruction algorithms to obtain the optimal parameters. The Q.clear algorithm with penalty function of β=200 and β=150 is recommended for brain neurological images of GE Healthcare PET/CT scanner.

Use your device to scan and read the article online

How to cite this article: Asami M, Aghahosseini F, Farzanehfar S, Ghafarian P, Salehi Y, Ay MR, Kasraie N, Sheikhzadeh P. Optimization of image reconstruction protocol in neurological [^{18}F]FDG brain PET imaging using BGO-based Discovery IQ Scanner. Iran J Nucl Med. 2025;33(2):103-115.

https://doi.org/10.22034/irjnm.2025.130021.1677

INTRODUCTION

Positron emission tomography (PET) plays an important role in diagnosing physiological function, molecular changes and pathological abnormalities [1]. PET/CT systems are able to show anatomical features, such as the location of lesions using CT and its metabolic changes with PET, at the same time [2]. PET image quality affects not only quantitative values but also visual interpretation. The quality of an image varies under the influence of the scanner model, protocol and reconstruction parameters [3]. In recent years, progress in reconstruction methods has noticeably improved the quality of PET images [4, 5]. One of the most widely used PET image reconstruction methods is the algorithm of Ordered Subset Expectation Maximization (OSEM). In this iterative statistical algorithm, the change in numbers of iterations and subsets, post-filters and with or without the use of PSF recovery, determines image quality [6]. OSEM however suffers from an inherent downside of being unable to attain full convergence due to elevated noise levels when increasing iteration times. OSEM algorithms are usually immaturely terminated after only a few iterations so as to avoid noise amplification, which may therefore lead to under-convergence and hence bias in quantifying the lesion.

Recently, Q. Clear, a Bayesian penalized likelihood (BPL) algorithm has been employed in PET/CT scanners of GE Healthcare to improve the quality of clinical images. This algorithm incorporates modeling of the point spread function (PSF) and introduces an additional compensation term to the conventional OSEM (Ordered Subsets Expectation Maximization) formulation. The mathematical expression of the algorithm is as follows:

$$X = \arg\max \sum_{i=1}^{n_d} y_i \log [p_x]_i - [p_x]_i - \beta R(x) \quad \text{Eq.1}$$

In this equation, yi denotes the measured coincidence data acquired by the PET system, represents the image estimate, and p is the system geometry matrix. The term R(x) serves as a regularization function to suppress noise. The only variable factor is the parameter β, modulates the relative weight of the regularization term in relation to the statistical contribution of the data. This approach facilitates the use of a higher number of iterations to achieve full convergence without substantially amplifying image noise [7].

As a result, in Q.Clear the possibility of full convergence of the image is realized and a more accurate quantification will be obtained compared to OSEM reconstructed images. Of course, excessive beta increase can cause smoothing, especially in small lesions [8, 9].

Wagatsuma et al. proposed optimal β values in BPL for brain PET using 3D Hoffman and cylindrical phantoms for Alzheimer's disease using two OSEM+TOF algorithms (under clinical conditions) and BPL+TOF(β=20-1000) reconstructions. They concluded that BPL performed better than OSEM in β ranges of 20-450 for [^{18}F]FDG and 20-600 for PiB (a C-11 tracer compound). Also, they performed a validation study using ten patients (five healthy patients and five Alzheimer's patients) for scoring. Their evaluators visually ranked β = 200 for [^{18}F]FDG and 450 for [^{11}C]PiB as being the most optimal among all images reconstructed with BPL. This study shows that contrast and noise both increase with decreasing β, demonstrating a need for balance between these two parameters, which the BPL algorithm (unlike OSEM), can establish this trade-off well [10].

In another study, Miwa et al. aimed to evaluate the detection of small lesions, with images taken using a NEMA phantom with OSEM+PSF, OSEM+TOF, OSEM+PSF+TOF, and BPL+PSF+TOF algorithms (with beta from 50 to 400) for reconstruction. The small hot spheres were evaluated quantitatively by recovery coefficient (RC) and detection index (DI) as well as visually. The result of this study determined that the BPL algorithm along with TOF can detect lesions smaller than 6 mm better than other types of reconstruction based on OSEM, and β = 200 was concluded as the optimal beta to detect hot lesions below one centimeter [9, 11].

Also, in part of the study by Reynés-Llompart et al., 5 clinical brain (neuro-oncological) images reconstructed with β=50-500, in steps of 50, were used to evaluate the optimal beta. Two experts were asked to evaluate the images in terms of the definition of the gyri and basal ganglia and the overall image quality. The results of this study showed that for brain images taken with the radiopharmaceutical [^{18}F]FDG and a BGO scanner, the optimal beta value is 100 to 200 [12].

Although many studies have in recent years appeared in the literature claiming to improve the reconstruction conditions of oncology images, the optimization of protocols for brain PET images warrants more studies, due to the new protocols of recent PET/CT cameras [3]. Our aim in this research was to evaluate parameters affecting the quality of brain PET images such as changes in the number of iterations and subsets, β values and with or without the use of PSF recovery, and

to determine the optimal values and reconstruction protocols to achieve optimally diagnostic parameters in the GE Healthcare PET/CT BGO-based scanners. Quantitatively, contrast, noise and resolution were evaluated. Additionally, noise, contrast and the overall quality of the image were visually and qualitatively also evaluated.

METHODS

Ethics approval and consent to participate

This article does not contain any studies with human participants or animals performed by any of the authors and is only a retrospective study. The anonymized patient's data were used in this study which approved by Research Ethics Committee of School of Medicine-IKHC, Tehran University of Medical Sciences (Approval code: IR.TUMS.IKHC.REC.1402.184).

PET-CT system

This study was conducted in the nuclear medicine department of Imam Khomeini Hospital, Tehran University of Medical Sciences, using a GE Discovery IQ PET-CT scanner (GE Healthcare, Waukesha, WI, United States). The PET scanner included bismuth germanate oxide (BGO) crystals, 5 PET detector rings and each ring included 36 detector blocks, diameter of 74 cm, transaxial FOV of 70 cm, and axial FOV of 26 cm. Along with the PET, a 16-slice CT scanner with 70 cm FOV reconstruction was used to correct for attenuation and scatter [13-15] .

Reconstruction algorithm

The obtained images were reconstructed using OSEM and BPL algorithms. In the OSEM algorithm, iterations (2-4-8-14-20), subsets (1-6-12) and 3.2 mm Gaussian filtration were used along with PSF recovery. Iteration-Subset=12-12 was routinely used to reconstruct the brain images of patients at the Imam Khomeini Nuclear Medicine Center. We reconstructed the images in this iteration-subset, once with a 6.4 mm Gaussian filter and once without PSF recovery. In the BPL algorithm, β=50-500 with 50 steps was used to reconstruct the images. Variations in the number of iterations and subsets in the Q.Clear, unlike the OSEM algorithm, are disabled in the GE Discovery IQ PET-CT scanner software.

Phantom study

We used a two-slice Hoffman phantom (Figure 1a) to draw and compare line profiles in different reconstruction parameters, a Carlson phantom to calculate COVand modified RC, and two point sources to obtain and compare FWHMs. Hoffman's phantom with a volume of 290 ml, contained parts of the gray matter of the brain. In similar articles that used a 1200 mL 3D Hoffmann phantom, 0.54 mCi of [^{18}F]FDG radiopharmaceutical were injected into the phantom [10]. Therefore, we used 0.166 mCi (net dose) of [^{18}F]FDG for our phantom. 30 minutes later, we imaged the phantom for 10 minutes in a single bed with the Brain protocol. Using ImageJ software, two line profiles were drawn on the reconstructed images of Hoffman's phantom. A long line profile on the gyrus on the right side of the brain and a short line profile, slightly larger than the width of a gyrus. We imported the obtained values into a spreadsheet to compare the profiles obtained from the long line profile and obtain the ratio of the maximum value to the minimum value in different reconstruction conditions from the values of the short line profile. We filled a Carlson phantom((Figure 1b) made of acrylic, with an inner diameter of 20.32 cm, an outer diameter of 21.59 cm, and a length of 30.48 cm [16] with water and a net dose of 2.175 mCi (80.47 MBq) of [^{18}F]FDG. Carlson phantoms can be useful for evaluating properties such as tomographic uniformity, image contrast, noise and linearity. The volume of our phantom was 5700 ml. Therefore, the active concentration was calculated to be 11.3 kBq/cc (At the time of imaging). This phantom includes a uniform part, 9 pairs of hot sphere inserts with diameters of 4.7, 5.9, 7.3, 9.2, 11.4, 14.3, 17.9, 22.4 and 38.5 mm [17] and seven cold spheres with diameters of 5.9, 7.3, 9.2 , 11.4, 14.3, 17.9 and 22.3 mm [16]. We imaged the phantom in 2 Beds with 4 min per bed duration. Quantitative parameters employed for evaluating our images were COV and modified RC. To calculate the noise, from the uniform part of the phantom, 5 slices were selected and 60 ROIs (12 ROIs in each slice) were drawn, each with a diameter of 30 mm. COV percentage was calculated using the following formula:

$$COV = \frac{\mathrm{SD}_{(nROI)}}{mean_{(nROI)}} \times 100 \qquad \text{Eq.2}$$

where $\mathrm{SD}_{(nROI)}$ and $\mathrm{mean}_{(nROI)}$ are the standard deviation of the voxel values within the nROI, and mean nROI activity within the 60 ROIs respectively.

In the Hot spheres section, ROIs were drawn to the diameter of the spheres (9 ROIs were drawn for one of the two pairs of spheres). Using the following formula, we calculated the value of modified RC:

$$\text{modified } RC = \frac{mean\ activity\ concentration_{(HS)}}{true\ activity\ concentration} \quad \text{Eq.3}$$

where the mean activity concentration$_{(HS)}$ is the activity concentration in each hot sphere, and the true activity concentration is the real activity concentration (11.3 kBq/cc).
We used two capillary tubes (Figure 1c) to obtain FWHM. We filled the tips of the tubes with a small drop of radioactivity and took images of the tubes in the center and at a distance of 20 cm from the center of the gantry. Vertical and horizontal line profiles were drawn on point sources and FWHM was obtained from the average FWHM of horizontal and vertical line for each point.

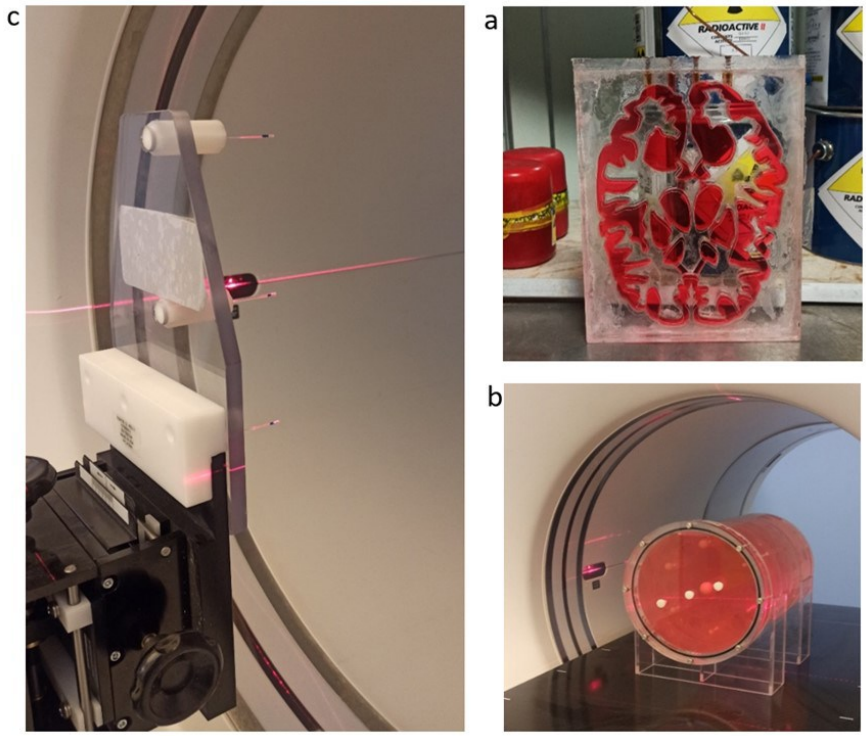

Figure 1. A two-slice Hoffman phantom (a) Carlson phantom (b) and capillary tubes (c)

Clinical study and visual analysis

In this study, 9 clinical images of patients (4 women and 5 men) who were referred for epilepsy or seizure imaging from Feb 2022 to Jan 2023 were used retrospectively. The objective of this study was to optimize neurological brain PET imaging. Accordingly, PET scans from patients with epilepsy and seizure disorders were utilized to ensure that the analysis focused exclusively on non-tumoral brain images, thereby eliminating potential confounding effects of tumoral pathologies. The weight of the patients ranged between 19 and 114 kg and their height spanned between 1.07 and 1.81 meters. Patients received an average of 4.75(±1.31) MBq/kg of [^{18}F]FDG. Approximately 45 minutes after intravenous injection, they were imaged for 30 minutes. To calculate the contrast, according to previous studies, we needed a hot lesion or spot and a homogeneous region with almost uniform absorption as background [18]. We selected the parts of the putamen and caudate as the hot spot, and the central region of the brain (left and right ventricles) as the background and drew the ROI. Then we obtained the contrast according to the following formula:

$$Contrast = \frac{ROI_{(hot\ spot)}}{ROI_{(background)}} \quad \text{Eq.4}$$

The above formula was used to evaluate putamen-to-background and caudate-to-background ratios. Also, to calculate the maximum to minimum ratio (as we did in the Hoffmann phantom), we drew a small line profile, slightly larger than the width of the caudate. Two nuclear medicine physicians were asked to review and score the images of nine patients blindly in terms of noise, contrast and overall image quality. Scoring was ranked according to a 5-point Likert scale (1 being the worst, 5 being excellent) for each set of reconstruction methods.

Statistical analysis

Sample t-test was used to compare and evaluate the results of two OSEM and Q.Clear reconstructions, or two different βs, with a value of P<0.05, and the Kappa Statistic test was used to evaluate the agreement between the two evaluators. In addition, by using the following formula, we obtained the relative difference of the results obtained from all types of reconstruction parameters together or with the value of iteration-subset=12-12, which was previously used to reconstruct the brain PET images of patients in the hospital [14].

$$\Delta feature_{(a-b)}\% = \frac{feature_b - feature_a}{feature_a} \times 100 \qquad \text{Eq.5}$$

Cost Function is used as an important tool in optimization problems and gives us the most optimal results [19]. Although all the parameters evaluated could be compared and evaluated individually, we used a cost function for the overall evaluation. Therefore, we used the cost function based on the following formula to calculate the optimal quantitative reconstruction parameter. Our nuclear medicine specialists deem resolution to be more important, contributing more to the interpretation of PET brain images. As a result, we gave FWHM a weight of 60% and for the rest of the parameters, we divided the weight of 40% equally.

$$Cost\ Function = \frac{\%60}{FWHM} + \%40[\frac{1}{COV} + \frac{1}{SOR} + RC + \frac{Putamen}{Background} + \frac{Caudate}{Background} + \frac{Max}{Min}(patient) + \frac{Max}{Min}(hoffman)] \qquad \text{Eq.6}$$

RESULTS

The line profiles obtained from different reconstruction parameters of the Hoffmann phantom show that β=50 had the most changes in the edge (Figure 2a). This chart clearly demonstrates that as the β value increases, the edges appear smoother. Moreover, there is a noticeable difference in edge representation between β=50-200 and the two-line profiles associated with the OSEM algorithm. Also, the highest values of the Max/Min ratio in the values obtained from the small line profile correspond to β=50-200 and iteration-Subset=12-20 (Figures 2b and 2c). As seen in Figure 3a, as β increases and the number of iteration × subset decreases, the amount of COV incrementally decreases. β=50 has more noise than It-S=12-12.

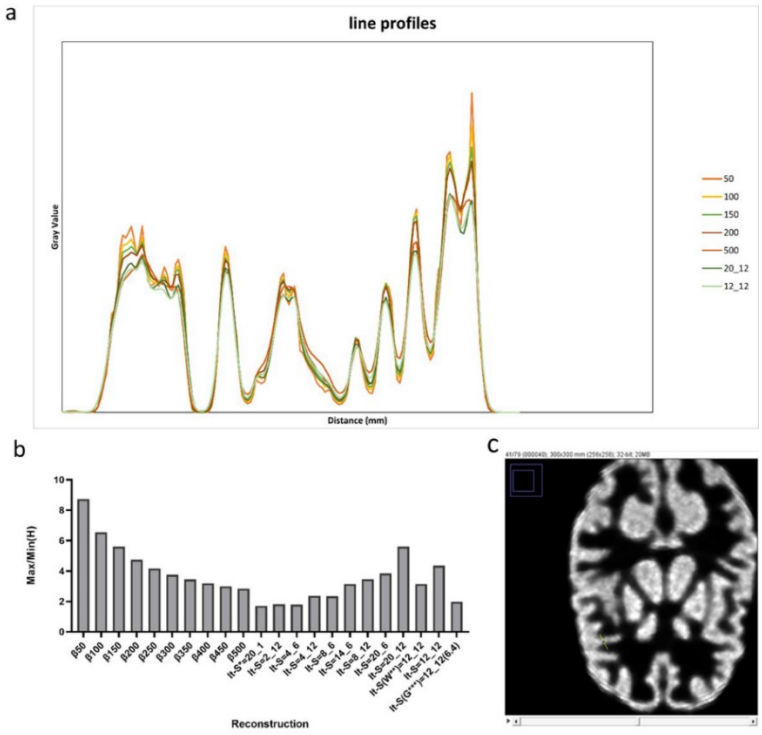

Figure 2. Comparison of the profiles of some reconstruction parameters obtained from Hoffman's phantom. The most changes are observed at beta=50 (a). The chart of the ratio of the maximum value to the minimum value in the Hoffmann phantom. The highest value of the Max/Min ratio in the numbers obtained from the small line profile corresponds to β=50-200 and iteration-Subset=12-20 (b) Short line profile on one of the gyri of the Hoffmann phantom (c)
*It=iteration, S=subset, **W=without PSF recovery, ***G=Gaussian

Table 1 shows the differences in COV of some reconstruction parameters compared to the COV in images reconstructed using It-S=12-12.
As the size of hot spheres become larger, the RC value however increases. The highest value of modified RC belongs to β=50-200(0.68) (Figure 3b). The reduction of RC from β=50 to β=500 is 24.68% (p<0.0002) on average. See the RC difference of some reconstruction parameters with It-S=12-12 in Table 1.

Table 1. Percentage difference in COV and RC for various reconstruction parameters

Beta (β)	%ΔCOV (vs. 12/12)	%ΔRC (vs. 12/12)
50	2.51%	18.99%
100	-0.76%	14.07%
150	-2.23%	9.06%
200	-3.33%	6.58%
Iteration-subset		
20-6	-1.23%	-3.87%
20-12	3.56%	10.38%

Note: All comparisons are made with iteration-subset=12-12.
%ΔCOV=(A-B), %ΔRC=((A-B)/B)×100
Where A is the parameter of interest and B is the reference (12-12).

Figure 3c shows the results of FWHM in all reconstruction conditions. FWHM was the lowest at all β values (β=50 to β=500: 3.36 to 3.41 mm). The value of FWHM from β=50 to β=500, in the central point source (D=0 cm), increased by 1.67%. The average FWHMs of the BPL algorithm at D=0 cm is 17.37% lower than It-S=12-12(4.1mm). It-S=12-12 without PSF recovery at D=0 cm has a 20.77% higher FWHM than It-S=12-12.
The average ratio of caudate to background, putamen to background, and maximum to minimum (corresponding to the line profile drawn on the caudate) in all patients can be seen in Figure 4. The highest value in all three ratios corresponds to β=50-150 and It-S=20-12. Figure 5A shows the results obtained from the mentioned Cost Function to evaluate the optimal parameter of quantitative reconstruction. According to the obtained numbers, β=50-200 and It-S=20-12 have higher values than It-S=12-12. Among all the images, reconstructed images with β=50-200 and It-S=12-12, 20-12 were blindly presented to two nuclear medicine experts.
The evaluators checked the images in terms of noise, contrast and overall image quality. The inter-observer correlations between readers for all three parameters evaluated using Cohen's kappa statistic can be summarized in Table 2. Visual scoring was also consistent with our quantitative analysis. Both evaluators agreed that β=50 and It-S=20-12 had the highest amount of noise, respectively. In 88.88% of cases, the first reader found the lowest amount of noise to be related to β=200, and the second reader was related to β=200 in 100% of cases. While considering the most preferred image in the reconstruction method we used, the best contrast was related to β=50 and β=100 for the first reader and β=100 for the second reader. The first reader found the lowest amount of contrast for β=200 and the second reader for β=50 and β=200. The highest score for the overall image quality for the first reader was β50 and β=150 in 100% and 88.89% of cases, respectively, and for the second reader it was β=200 and β=150 in 100% of cases. The lowest score for the overall image quality for the first reader was It-S=12-12, and for the second reader it was It-S=12-20.

DISCUSSION

This study was carried out for brain PET/CT neurological images with [18F]FDG, in a BGO-based system, in order to obtain the most optimal reconstruction parameters while comparing OSEM and BPL algorithms quantitatively and qualitatively. Considering that the algorithm used to reconstruct PET brain images in our Hospital was It-S=12-12, most of our comparisons were made with this parameter.
In the study of Wagatsuma et al. increasing beta and reducing the number of Iteration×Subset, reduces the COV [10].They reported that, unlike OSEM, the BPL algorithm provides a good balance between high contrast and low image noise. As previously explained in Eq1, beta is a factor that controls the balance between smoothing and edge suppression. This approach facilitates the use of a higher number of iterations to achieve full convergence [20].
As a result, in Q.Clear a more accurate quantification will be obtained compared to OSEM reconstructed images. The phantom evaluation of the present study showed that in most βs, the COV was lower than It-S=12-12, except for β=50 (Table 1; Figure 3a).

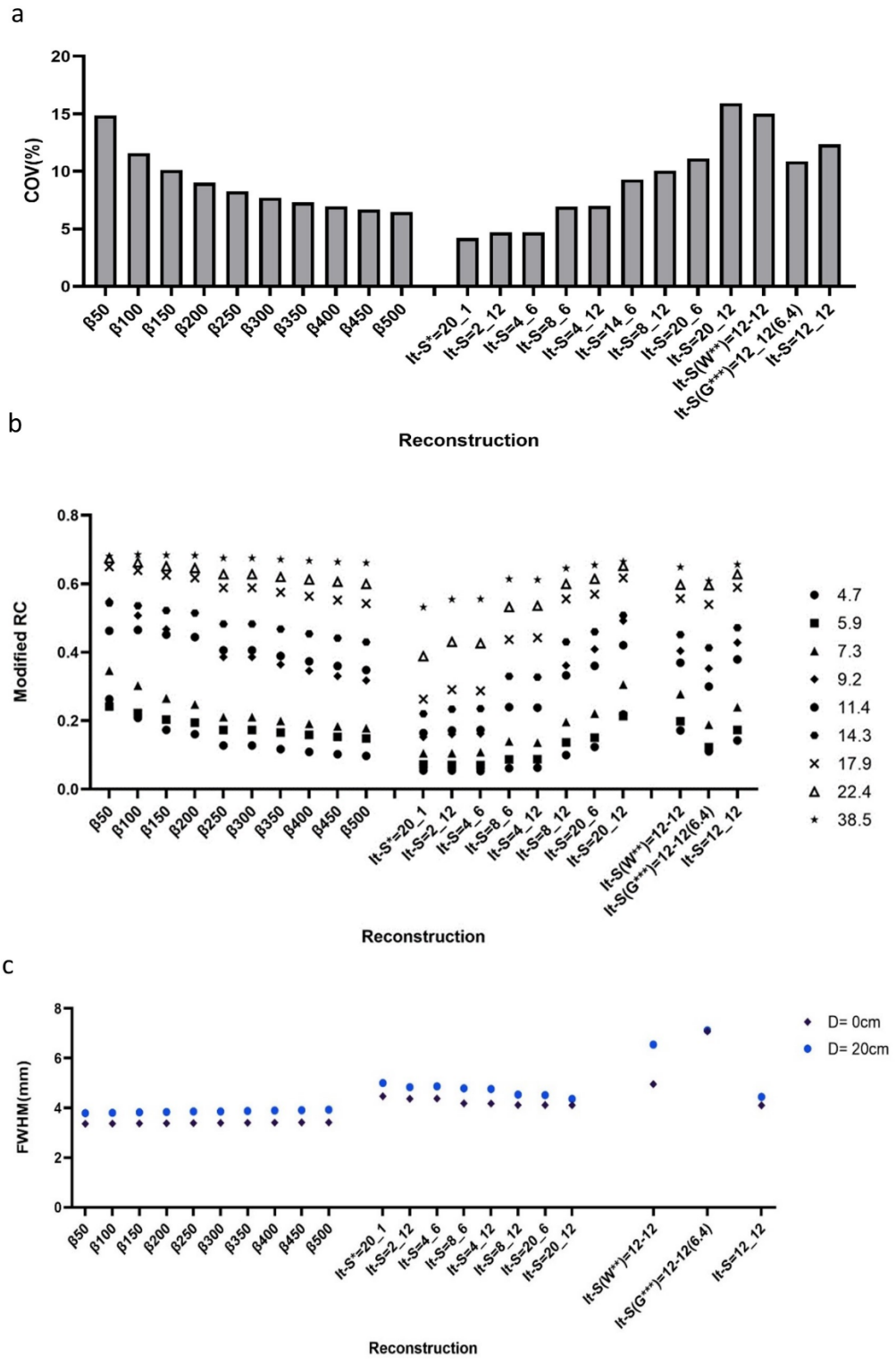

Figure 3. Quantitative evaluation of reconstruction parameters: (a) Coefficient of Variation (COV), (b) Recovery Coefficient (RC) in hot spheres of different sizes, and (c) Full Width at Half Maximum (FWHM) at the center and 20 cm off-center. Increasing β and reducing iteration × subset generally reduced COV. As the size of hot spheres become larger, the RC value however increases. The highest value of modified RC belongs to β=50-150. FWHM was the lowest at all β values
*It = iteration, S = subset, **W = without PSF recovery, ***G = Gaussian

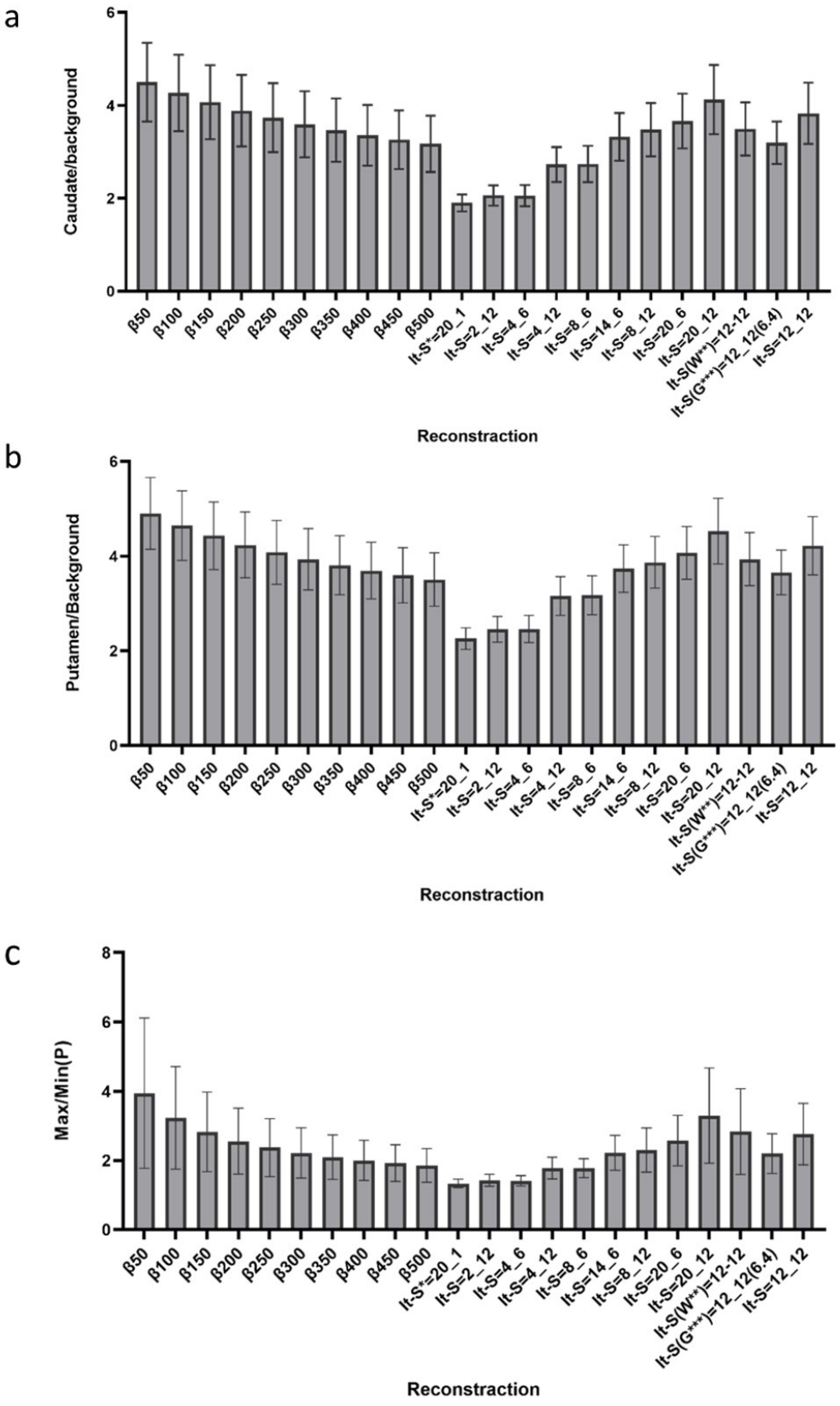

Figure 4. The average ratio of caudate to background, putamen to background, and maximum to minimum in all patient. The highest value in all three ratios corresponds to β=50-150 and It-S=20-12.
*It = iteration, S = subset, **W = without PSF recovery, ***G = Gaussian

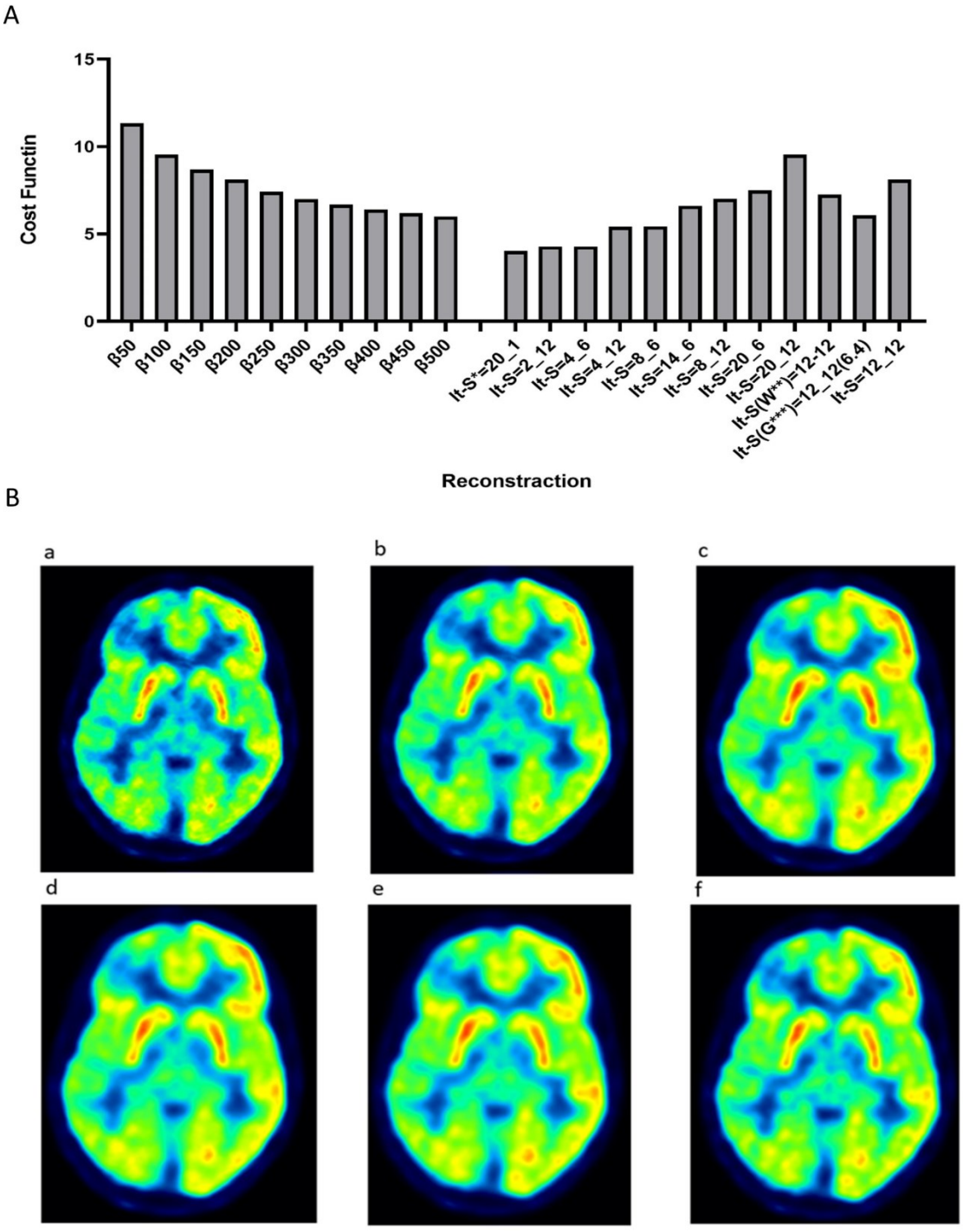

Figure 5. Evaluation of reconstruction parameters using (A) cost function values and (B) clinical images from a patient. Higher cost function values were observed for β=50–200 and It–S=20–12.
These six reconstruction conditions are shown in (B) in the following order: β = 50 (a), β = 100 (b), β = 150 (c), β = 200 (d), It–S = 12–12 (e), and It–S = 20–12 (f).
*It=iteration, S=subset, **W=without PSF recovery, ***G=Gaussian

Table 2. Clinical evaluation of inter-rater agreement and ratings of noise, contrast and overall IQ

Parameters	Highest ranked reconstruction (4 or 5) (% of cases)		Lowest ranked reconstruction (1 or 2) (% of cases)		Agreement	k
	Scorer 1	Scorer 2	Scorer 1	Scorer 2		
Noise	β =50, It-S=20-12 (100%, 55.56%)	β =50, It-S=20-12 (100%, 44.44%)	β =200 (88.88%)	β =200 (100%)	Moderate	0.511
Contrast	β =50, β100 (100%, 100%)	β =100 (100%)	β =200 (44.44%)	β =50, β=200 (44.44%, 33.33%)	Moderate	0.607
Overall IQ	β =50, β150 (100%, 88.89%)	β =200, β=150 (100%, 100%)	It-S=12-12 (11.11%)	It-S=20-12 (22.22%)	Moderate	0.508

This problem is stated in the study of Sadeghi et al. as that in low beta values, despite accurate quantification, image quality is compromised due to high noise values [21].

According to the Japanese Society of Nuclear Medicine (JSNM) criterion, which states that the acceptable noise level for images is below 15% [10], the COV value is within the acceptable range in all reconstruction conditions except when 20 iterations and 12 subsets were used. It-S=20-12, has more number of iteration × subset, higher COV, higher modified average RC and better cost function than It-S=12-12. The COV level exceeds 15% in It-S=20-12, similar to the condition in which PSF recovery is disabled.

PSF recovery reconstruction modeling effectively places the response lines at their true geometric locations. This algorithm compensates for partial volume effects, reduces parallax artifacts, and restores resolution, resulting in more accurate image estimation [22]. As shown in Figure 3c, the FWHM value is lower when PSF recovery is enabled compared to when it is disabled. Prieto et al. showed that algorithms that use PSF recovery have approximately 2-5% less noise than other algorithms. Their study reported when PSF recovery is incorporated into the reconstruction process, image contrast increases significantly. Moreover, the contrast-to-noise ratio was found to be 40% higher for iterations greater than five when images were reconstructed with PSF recovery [5]. Therefore, disabling the PSF recovery not only increases the noise, but also reduces the resolution and contrast of the images. As β increases, the FWHM of the point source also increases. However, our results indicate that BPL outperforms the OSEM algorithm in visualizing small active regions, since, as previously mentioned, it allows for an increased number of iterations to achieve full convergence and as shown in Figure 3c, the amount of FWHM in all values of BPL algorithm is lower than OSEM. The average modified RC, in all spheres, shows that β=50-250 have higher values than It-S=12-12.

While increasing the Gaussian filter reduces the COV in the It-S=12-12, it concurrently causes an approximate 70% increase in the FWHM. The maximum-to-minimum ratio, as well as the putamen-to-background and caudate-to-background ratios, decrease with increasing filter size. Thus, although increasing the Gaussian filter effectively reduces image noise, it also leads to a degradation in spatial resolution and contrast. In this regard, the study by Prieto et al. demonstrated that increasing the filter width leads to a decrease in contrast recovery, deviating from the true contrast values. They reported that when the filter width is less than 4 mm, the CNR values vary across different algorithms, whereas this difference disappears at greater filter widths [5].

Although all the parameters evaluated could be compared and evaluated individually, we used a cost function for the overall evaluation. By using a cost function, we obtained optimal quantitative values for reconstructing brain images. The comparison criterion was It-S=12-12. According to the results of the cost function, the images related to β=50-200, It-S=12-12, 20-12 were blindly presented to two nuclear medicine specialists to rank contrast and image quality from 1:worst to 5:best, and similarly, in terms of noise Score 1: the most to 5: the least, as per a Likert scale. According to the evaluators, due to the observation of a ringing artifact in β=50 images, it was decided to exclude this reconstruction parameter from the visual evaluation (Figure 5B). As a result, while announcing the scores of this parameter, we evaluated another related parameters. The results of visual evaluations show that β=200 has the lowest noise and the lowest contrast. Although, visually, among the 6 presented images, the specialists rated the contrast of the images reconstructed with It-S=12-12 higher than those reconstructed with β=200, they agreed that β=200 achieved a better balance between noise level and contrast compared to It-S=12-12. The first evaluator in 100% of cases and the second evaluator in 77.78% of cases believed that the overall quality of the image in β=200 scores 4 or 5. Moreover, based on the quantitative results, the contrast values for all parameters, including the caudate-to-background ratio, putamen-to-background ratio, and the maximum-to-minimum ratio in both the Hoffman phantom and patient images, were higher for β=200 compared to It-S=12-12. Therefore, according to the quantitative and qualitative results of clinical images, and considering the artifacts observed in the images reconstructed with β=50, this study recommends β=150 and β=200 as the optimal values for brain PET image reconstruction. Our results are consistent with the results of the study by Reynés-Llompart et al., which similar to ours, was conducted using a BGO-based scanner, five brain images reconstructed with different beta values were evaluated and scored by two experts. Their visual assessment, focusing on the definition of the gyri and basal ganglia as well as overall image quality, indicated that β=100-200 achieved the highest scores. However, our study has evaluated this aspect through both quantitative and qualitative analyses [12].

In the study by Wagatsuma et al., the optimal beta value for brain image reconstruction using [^{18}F]FDG was β=100-300 based on quantitative assessments, and β=200 was recommended based on visual evaluations [10].

As a result of this optimization, an overall image quality improvement can be considered and implemented for BGO scanners using these values compared to the conventional OSEM reconstruction method; i.e. Q.Clear's BSREM method can be harnessed to lower scan times or patient injected activity vis a vis patient comfort and reduced radiation exposure.

Our study was not exempt from limitations, the first of which was our small sample size; due to the small number of images of patients and scorers, the optimal parameter may vary with the increase of either one. Therefore further studies (preferably multi-centric) are needed to ascertain the validation of the clinical value of BPL to OSEM brain PET. Also, due to the different appearance of Q.Clear images compared to OSEM and the existence of ringing artifacts in β=50 images, it was not possible to review the images completely blindly, and this may have caused reader bias. Although our readers were blinded to the type of reconstruction we presented them, it can be hypothesized that an experienced reader may be able to recognize the actual algorithm used based on the reconstructed images [23] and finally, we examined the optimal β value candidates of BGO PET scanners using only the standard [^{18}F]FDG radioisotope. However amyloid tracers such as [^{18}F]-florbetapir, [^{18}F]-florbetaben, and [^{18}F]-flutemetamol are also commonplace. The β value for such tracers must therefore also be studied and optimized on BGO type systems since the injected doses, uptake, and acquisition times will vary accordingly [24]. Furthermore, the effective recovery performance of PSF algorithms may call for further in-depth examination.

As Wagatsuma et al. remarked, although PSF algorithms recover spatial resolution and highlight hot lesions, some institutions do not apply it to reconstructed clinical images as the algorithm may induce edge artifacts. Prieto similarly contends that PSF algorithms should not be applied to radioisotopes with diffuse cortical uptake such as [^{18}F]FDG to avoid overshooting the edge of the cortex. Also, although our readers were blinded to the type of reconstruction we presented them, it can be hypothesized that an experienced reader may be able to recognize the actual algorithm used based on the reconstructed images [17].

CONCLUSION

Phantom and neurological brain images taken with GE Healthcare PET/CT scanner were reconstructed using different algorithms and parameters. Quantitatively, the parameters of FWHM, COV, modified RC, putamen to background ratio, caudate to background ratio and maximum to minimum ratio of line profile in Hoffman phantom and clinical images were obtained. The parameters were put in a cost function and quantitatively, β=50-200 and It-S=20-12 had better results. This study recommends β=200 and β=150 for reconstructing brain images according to the quantitative results and visual inspections.

Acknowledgements

This study has been granted funding by Tehran University of Medical Sciences with grant number 1402-3-101-67958. We acknowledge support from the Department of Nuclear Medicine at Imam Khomeini Hospital Complex, Tehran, Iran.

REFERENCES

1. Ikari Y, Akamatsu G, Nishio T, Ishii K, Ito K, Iwatsubo T, Senda M. Phantom criteria for qualification of brain FDG and amyloid PET across different cameras. EJNMMI Phys. 2016 Dec;3(1):23.
2. Pelosi E, Messa C, Sironi S, Picchio M, Landoni C, Bettinardi V, Gianolli L, Del Maschio A, Gilardi MC, Fazio F. Value of integrated PET/CT for lesion localisation in cancer patients: a comparative study. Eur J Nucl Med Mol Imaging. 2004 Jul;31(7):932-9.
3. Akamatsu G, Ikari Y, Nishio T, Nishida H, Ohnishi A, Aita K, Sasaki M, Sasaki M, Senda M. Optimization of image reconstruction conditions with phantoms for brain FDG and amyloid PET imaging. Ann Nucl Med. 2016 Jan;30(1):18-28.
4. Yoshii T, Miwa K, Yamaguchi M, Shimada K, Wagatsuma K, Yamao T, Kamitaka Y, Hiratsuka S, Kobayashi R, Ichikawa H, Miyaji N, Miyazaki T, Ishii K. Optimization of a Bayesian penalized likelihood algorithm (Q.Clear) for 18F-NaF bone PET/CT images acquired over shorter durations using a custom-designed phantom. EJNMMI Phys. 2020 Sep 11;7(1):56.
5. Prieto E, Martí-Climent JM, Morán V, Sancho L, Barbés B, Arbizu J, Richter JA. Brain PET imaging optimization with time of flight and point spread function modelling. Phys Med. 2015 Dec;31(8):948-955.
6. Akamatsu G, Ishikawa K, Mitsumoto K, Taniguchi T, Ohya N, Baba S, Abe K, Sasaki M. Improvement in PET/CT image quality with a combination of point-spread function and time-of-flight in relation to reconstruction parameters. J Nucl Med. 2012 Nov;53(11):1716-22.
7. Ross S. Clear white paper. Chicago, IL: GE Healthcare. 2014. [cited 13 June 2025]. Available at: https://www.gehealthcare.com/en-sg/-/jssmedia/widen/2018/01/25/0204/gehealthcarecom/migrated/2018/03/22/0155/ocuments-us-global-products-pet-ct-whitepaper-q-clear-ge-healthcare-white-paper_qclear_pdf.pdf?rev=-

1&srsltid=AfmBOopJ24FeLlHDtYrLM-UlNvjbwRNEdftz_44nzF_6rGYBdNjO8-Sp

8. Teoh EJ, McGowan DR, Macpherson RE, Bradley KM, Gleeson FV. Phantom and Clinical Evaluation of the Bayesian Penalized Likelihood Reconstruction Algorithm Q.Clear on an LYSO PET/CT System. J Nucl Med. 2015 Sep;56(9):1447-52.
9. Miwa K, Yoshii T, Wagatsuma K, Nezu S, Kamitaka Y, Yamao T, Kobayashi R, Fukuda S, Yakushiji Y, Miyaji N, Ishii K. Impact of γ factor in the penalty function of Bayesian penalized likelihood reconstruction (Q.Clear) to achieve high-resolution PET images. EJNMMI Phys. 2023 Jan 22;10(1):4.
10. Wagatsuma K, Miwa K, Kamitaka Y, Koike E, Yamao T, Yoshii T, Kobayashi R, Nezu S, Sugamata Y, Miyaji N, Imabayashi E.. Determination of optimal regularization factor in Bayesian penalized likelihood reconstruction of brain PET images using [18F] FDG and [11C] PiB. Med Phys. 2022;49(5):2995-3005.
11. Miwa K, Wagatsuma K, Nemoto R, Masubuchi M, Kamitaka Y, Yamao T, Hiratsuka S, Yamaguchi M, Yoshii T, Kobayashi R, Miyaji N, Ishii K. Detection of sub-centimeter lesions using digital TOF-PET/CT system combined with Bayesian penalized likelihood reconstruction algorithm. Ann Nucl Med. 2020 Oct;34(10):762-771.
12. Reynés-Llompart G, Gámez-Cenzano C, Vercher-Conejero JL, Sabaté-Llobera A, Calvo-Malvar N, Martí-Climent JM. Phantom, clinical, and texture indices evaluation and optimization of a penalized-likelihood image reconstruction method (Q.Clear) on a BGO PET/CT scanner. Med Phys. 2018 Jul;45(7):3214-3222.
13. Reynés-Llompart G, Gámez-Cenzano C, Romero-Zayas I, Rodríguez-Bel L, Vercher-Conejero JL, Martí-Climent JM. Performance Characteristics of the Whole-Body Discovery IQ PET/CT System. J Nucl Med. 2017 Jul;58(7):1155-1161.
14. Sadeghi F, Sheikhzadeh P, Kasraie N, Farzanehfar S, Abbasi M, Salehi Y, Ay M. Phantom and clinical evaluation of Block Sequential Regularized Expectation Maximization (BSREM) reconstruction algorithm in 68Ga-PSMA PET-CT studies. Phys Eng Sci Med. 2023 Sep;46(3):1297-1308.
15. Al-Fatlawi M, Pak F, Farzanefar S, Salehi Y, Monsef A, Sheikhzadeh P. Optimization of the Acquisition Time and Injected Dose of 18 F-Fluorodeoxyglucose Based on Patient Specifications for High-Sensitive Positron Emission Tomography/Computed Tomography Scanner. World J Nucl Med. 2023 Sep 6;22(3):196-202.
16. Demirkaya O, Al-Mazrou R, ASSURANCE ATIQ. Devices for evaluating imaging systems. Nuclear Medicine Physics: A Handbook for Teachers and Students: IAEA, Vienna; 2014. 550.
17. Sadremomtaz A, Taherparvar P. The influence of filters on the SPECT image of Carlson phantom. J Biomed Sci Eng. 2013 Mar 12;6(3):291-7.
18. Sanaat A, Akhavanalaf A, Shiri I, Salimi Y, Arabi H, Zaidi H. Deep-TOF-PET: Deep learning-guided generation of time-of-flight from non-TOF brain PET images in the image and projection domains. Hum Brain Mapp. 2022 Nov;43(16):5032-5043.
19. Sheikhzadeh P, Sabet H, Ghadiri H, Geramifar P, Ghafarian P, Ay MR. Design, optimization and performance evaluation of BM-PET: A simulation study. Nucl Instr Meth Phys Res A. 2019;940:274-82.
20. Jonmarker O, Axelsson R, Nilsson T, Gabrielson S. Comparison of Regularized Reconstruction and Ordered Subset Expectation Maximization Reconstruction in the Diagnostics of Prostate Cancer Using Digital Time-of-Flight 68Ga-PSMA-11 PET/CT Imaging. Diagnostics (Basel). 2021 Mar 31;11(4):630.
21. Sadeghi F, Sheikhzadeh P, Farzanehfar S, Ghafarian P, Moafpurian Y, Ay M. The effects of various penalty parameter values in Q.Clear algorithm for rectal cancer detection on 18F-FDG images using a BGO-based PET/CT scanner: a phantom and clinical study. EJNMMI Phys. 2023 Oct 16;10(1):63.
22. Akamatsu G, Ishikawa K, Mitsumoto K, Taniguchi T, Ohya N, Baba S, Abe K, Sasaki M. Improvement in PET/CT image quality with a combination of point-spread function and time-of-flight in relation to reconstruction parameters. J Nucl Med. 2012 Nov;53(11):1716-22.
23. Liberini V, Pizzuto DA, Messerli M, Orita E, Grünig H, Maurer A, Mader C, Husmann L, Deandreis D, Kotasidis F, Trinckauf J, Curioni A, Opitz I, Winklhofer S, Huellner MW. BSREM for Brain Metastasis Detection with 18F-FDG-PET/CT in Lung Cancer Patients. J Digit Imaging. 2022 Jun;35(3):581-593.
24. Lindström E, Oddstig J, Danfors T, Jögi J, Hansson O, Lubberink M. Image reconstruction methods affect software-aided assessment of pathologies of [18F] flutemetamol and [18F] FDG brain-PET examinations in patients with neurodegenerative diseases. Neuroimage Clin. 2020;28:102386.